Applied Radiation and Isotopes 170 (2021) 109634

Contents lists available at ScienceDirect

Applied Radiation and Isotopes

journal homepage: http://www.elsevier.com/locate/apradiso

A kinetic model for the thermoluminescent high dose response of LiF:Mg,Cu,P (MCP-N)

J.F. Benavente *, J.M. Gómez-Ros, V. Correcher

CIEMAT, Av. Complutense 40, E-28040, Madrid, Spain

ARTICLE INFO

Keywords:
Thermoluminescence
Kinetic model
Lithium fluoride
LiF:Mg,Cu,P
MCP

ABSTRACT

This contribution describes a kinetic model attempting to reproduce the response of the thermoluminescent material LiF:Mg,Cu,P when it is irradiated to absorbed dose values in the kGy range. The modelling is based on the hypothesis of a relationship between the irradiation time (i.e. the absorbed dose) and the density of trapping/recombination centres.

X-ray diffraction and thermal X-ray diffraction measurements have been performed to investigate the potential radiation and thermal damage on the structure of the material, including the possibility of partial phases. The proposed kinetic model qualitatively reproduces the observed changes in the TL glow curve for temperatures above the main peak as well as the two observed regions of absorbed dose response: linear and sub-linear.

1. Introduction

Thermoluminescence (TL) basic models (McKeever, 1985) assume that the concentrations of available trapping centres, N_i (cm^{-3}), and recombination centres, M (cm^{-3}), remain constant during the irradiation and readout processes, being dependent only of the dopants presence. However, several authors have shown that F - centres production, which is related to N_i values, as well as H - centres production, that is related to M values, can also be described as a defect production mechanism due to the interaction of ionizing radiation with ionic crystals (Schuldman and Compton, 1963; McKeever, 1985). Therefore, N_i and M values do not necessarily need to be considered constant during irradiation and a dynamic model can be proposed. In particular, the creation of F - centres in an ionic-crystal due to heavy ion irradiation has been already reported (Dauletbekova et al., 2014; Epie et al., 2016) following a sigmoid function.

LiF:Mg,Cu,P is a synthetic TL material, currently used in dosimetric applications, exhibiting two main specific characteristics related to the absorbed dose dependence: strong changes in the glow curve for temperatures above the main peak when it is irradiated to absorbed dose values higher than kGy; and sub-linear variation in the response curve after the first linear region (Moscovitch and Horowitz, 2007; Ginjaume et al., 1999).

The main objective of this contribution is to present a kinetic model combining the differential equation system describing the electron and hole traffic between valence/conduction bands and trapping/recombination centres (Benavente et al., 2020) with the growth of such a centres during irradiation following a sigmoid-type equation. As it will be shown below, this model qualitatively reproduces the observed behaviour and response of LiF:Mg,Cu,P.

2. Materials and methods

LiF:Mg,Cu,P samples (MCP-N, commercially produced at the IFJ, Krakow, Poland purchased to RADPRO International GmbH) were irradiated to very high absorbed dose values, ranged from 1 kGy to 1 MGy, using the ^{60}Co source in the NAYADE pool irradiation facility of CIEMAT (Carella and Hernández, 2015; García-Cortés et al., 2018). The TL glow curves were measured in a nitrogen atmosphere from room temperature to 400 °C using an automated RISØ TL/OSL model TL DA-12 reader equipped with an EMI 9635 QA photomultiplier and a blue filter (Melles-Griot FIB002) with wavelength is peaked at 320–480 nm and the peak transmittance is 60% with FWHM is 80 (16) nm. The incandescent background was directly subtracted from the TL glow curves.

Because of strong sensitivity loss of LiF:Mg,Cu,P has been reported when annealed at temperatures over 240 °C, only new, untreated samples have been employed and none of them has been reused. The transit absorbed dose that could have been integrated by the samples would be negligible compared with the irradiation values of 1 kGy and above.

The measurements were performed in the X-ray CAI unit of

* Corresponding author.
E-mail address: jf.benavente@ciemat.es (J.F. Benavente).

https://doi.org/10.1016/j.apradiso.2021.109634
Received 28 October 2020; Received in revised form 30 December 2020; Accepted 29 January 2021
Available online 5 February 2021

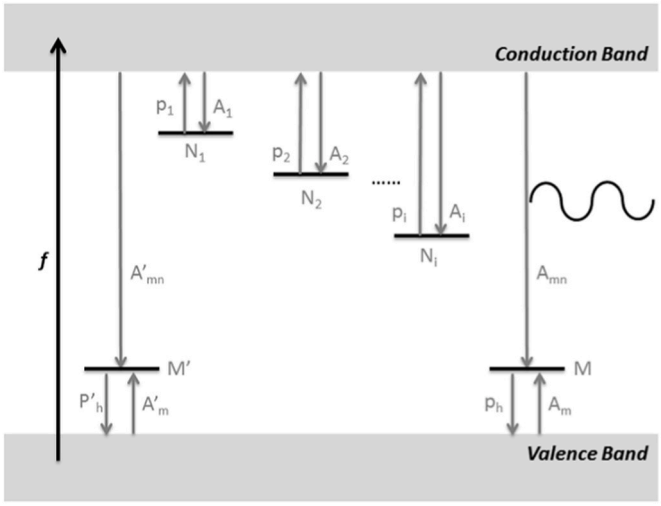

Fig. 1. Energy levels and allowed transitions scheme for the model described by the set of equation (1), consisting of i trapping centres (N_1, N_2 ... N_i) one radiative recombination centre (N_h) and one non-radiative recombination centre. During irradiation, electron-hole pairs will be created with a rate *f*, depending on the absorbed dose rate (see the text for additional details).

Universidad Complutense de Madrid (UCM, Spain), using a Bruker D8 Advance dust diffractometer, equipped with a highly stable X-ray source with copper anode and a SOL-X detector for dispersion of energy and a large active area for X-ray and thermal X-ray diffraction (XRD and TXRD). The diffractometer works in Bragg-Brentano geometry and has an automatic sample exchanger. The software used by the equipment for the acquisition, treatment and evaluation of diffractometric data is DIFFRACplus.

For the modelling of the TL emission, the set of trapping centres and two competing recombination centres (one radiative and the other non-radiative) schematically shown in Fig. 1, together with the allowed transitions has been considered. The corresponding set of differential equations as follows (Benavente et al., 2020):

$$\dot{n}_c = f + \sum_{i=1}^{N} p_i n_i - n_c \left[\sum_{i=1}^{N} A_i (N_i - n_i) + A'_m m' + A_m m \right] \quad (1)$$

$$\dot{n}_i = -p_i n_i + A_i (N_i - n_i) n_c$$
$$\dot{m}' = A'_m (M' - m') - A'_{nm}\, m\, n_c - p'_h\, m'$$
$$\dot{m} = A_m (M - m)\, n_h - A_{nm}\, m\, n_c - p_h\, m$$
$$\dot{n}_h = f - A'_m (M' - m')\, n_h + p'_h\, m' - A_m (M - m)\, n_h + p_h\, m$$

where:

n_c is the electron concentration in the conduction band (cm^{-3}).

n_i is the electron concentration in the trapping centres i (cm^{-3}).

m' is the hole concentration in the non-radiative recombination centres (cm^{-3}).

m is the hole concentration in the radiative recombination centres (cm^{-3}).

n_h is the hole concentration in the valence band (cm^{-3}).

N_i is the total density of electron trapping centres i (cm^{-3}).

M′ is the total density of non-radiative recombination centres (cm^{-3}).

M is the total density of radiative recombination centres (cm^{-3}).

f is the rate of production of electron-hole pairs during irradiation ($cm^{-3}s^{-1}$).

A_i is the probability factor for the electron trapping centres i (cm^3s^{-1}).

A'_h is the probability factor for the non-radiative recombination centres (cm^3s^{-1}).

A_h is the probability factor for the radiative recombination centres (cm^3s^{-1}).

A'_{mn} is the non-radiative recombination probability (cm^3s^{-1}).

A_{mn} is the radiative recombination probability (cm^3s^{-1}).

$p_i = s_i \exp(-E_i/kT)$; s_i is the frequency factor (s^{-1}), E_i is the activation energy (eV) for electron trapping centres i

$p'_h = s'_h \exp(-E'_h/kT)$; s'_h is the frequency factor (s^{-1}), E'_h is the activation energy (eV) for the nonradiative recombination centres

$p_h = s_h \exp(-E_h/kT)$; s_h is the frequency factor (s^{-1}), E_h is the activation energy (eV) for the radiative recombination centres.

T is the temperature (K).

K is the Boltzman's constant (8.617×10^{-5} eV/K).

This differential equations system has not an analytical solution but it has been solved using a numerical Runge – Kutta – Fehlberg (RKF45) algorithm (Cheney and Kincaid, 2002). Nevertheless, the model described by equation (2) only considers the effect of irradiation through the rate of production of electron-hole pairs, *f*, without considering the possibility of changes in the density of either trapping or recombination centres. To take it into account, a hypothetical dependence of N and M values on the irradiation time using the Gompertz sigmoid function has been introduced:

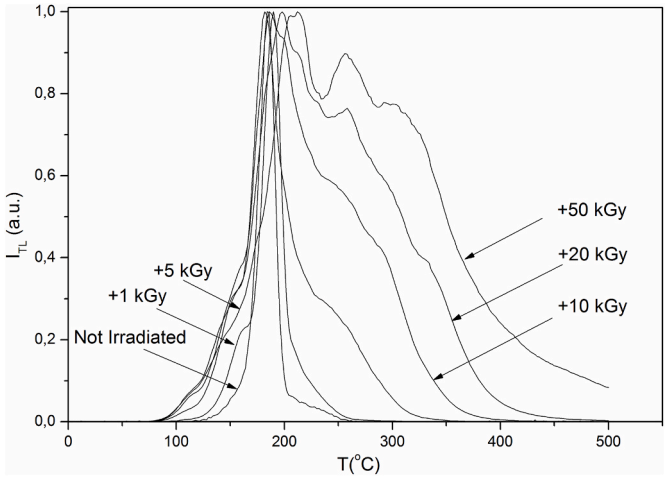

Fig. 2. Induced TL glow curves from different aliquots of LiF:Mg,Cu,P samples irradiated in the range of 1 kGy to 50 kGy (each glow curve is normalized to its the maximum). Note the increase of the TL intensity over 200 °C with dose.

$$N(t) = N_{sat} \exp\left[-\log\left(\frac{N_{sat}}{N_0}\right) e^{-C\ t} \right] \quad (2)$$

where:

N_0 (cm^{-3}) is the density of trapping/recombination centres initially available, i.e. those centres created by dopants.

N_{sat} (cm^{-3}) is the saturation density of trapping/recombination centres, i.e., the asymptotic value of the function, $N_{sat} = N(t \to \infty)$.

C (s^{-1}) is a constant value characterizing the growth rate of centres density during irradiation time.

t (s) is the irradiation time.

N(t) is the density of trapping/recombination centres after an irradiation time, t. Therefore, N(t) depends both on the initial density due to dopants, N_0, as well as those created during irradiations. The Gompertz equation (2) permits to describe the time variation in the density of either trapping or recombination centres, as a function of the initial density of centres, the parameter C and the saturation value, N_{sat}. This model avoids an unlimited increase of density N(t) that would give unrealistic big values during the simulations.

A sigmoid-type function like equation (2) is similar to those used to describe the creation of F - centres in ionic-crystal during heavy ion irradiation. It has a slow growth at the starting and ending stages during the irradiation period. Thus, the evolution of the density of trapping/recombination centres during irradiation is governed by the three corresponding parameters (N_0, N_{sat}, C).

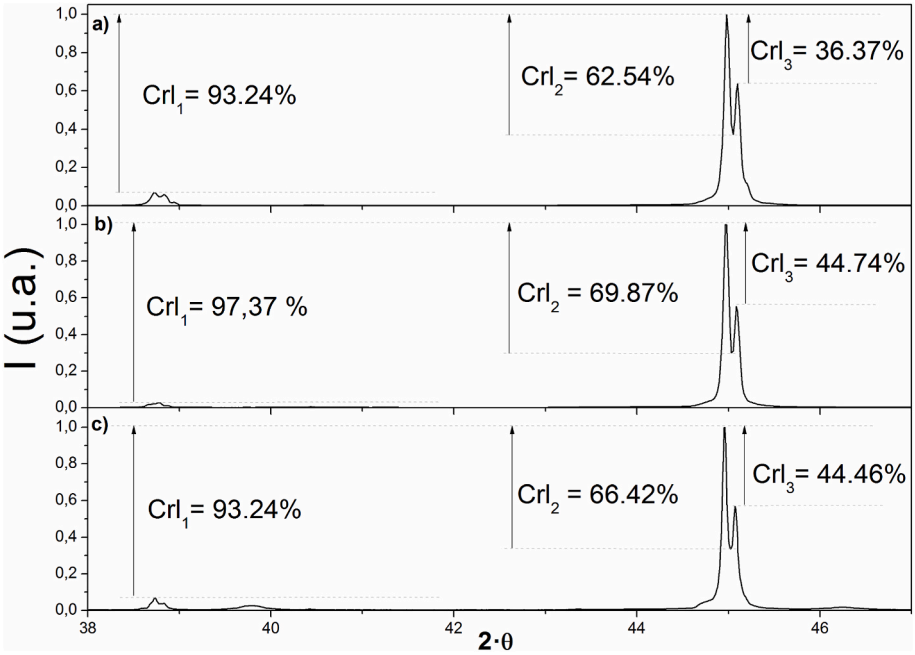

Fig. 3. X-ray diffraction (XRD) patterns corresponding to a) irradiated at 1 kGy, b) irradiated at 20 kGy and c) unirradiated samples, showing the crystallinity index values.

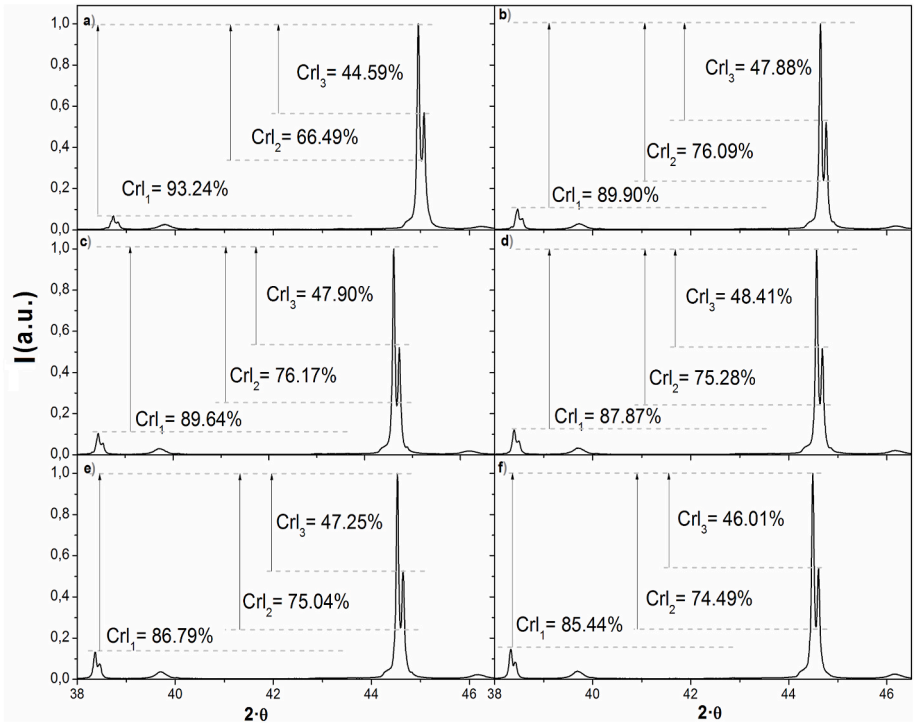

Fig. 4. Thermal X-ray diffraction (TXRD) patterns of unirradiated sample at six different temperatures a) 25 °C, b) 200 °C, c) 220 °C, d) 240 °C, e) 260 °C, f) 280 °C, showing the crystallinity index values.

3. Results and discussion

Fig. 2 shows the TL glow curves from LiF:Mg,Cu,P samples irradiated to six increasing absorbed dose values. As it can be seen, in addition to the signal appearing below 240 °C for 1 kGy, higher temperature contributions appear when the absorbed dose increases. These results agree with those previously reported by other authors (Bilski et al., 2008). In all the cases, the TL glow curves were measured by heating the samples up to temperatures higher than those usually employed by dosimetry services in routine applications, where the main objective is the reusability of the LiF:Mg,Cu,P. Nevertheless, the more significant changes in the TL glow curves are observed above the 200 °C, when the traps usually acting as electrons sink for low temperatures start to release electrons (Benavente et al., 2020).

Both XRD and TXRD measurements have been performed to determine the potential effect of the radiation and temperature on the lattice

Table 1
Kinetic parameters for the trapping centres in the LiF:Cu,Mg,P model.

trap ID	E (eV)	s (s^{-1})	A (cm^3s^{-1})	N_0 (cm^{-3})	N_{sat} (cm^{-3})	C
I	1.28	5.3×10^{11}	10^{-8}	1×10^8	3.25×10^{11}	4.00×10^{-6}
II	1.28	1.8×10^{14}	10^{-8}	1×10^8	3.25×10^{11}	1.00×10^{-5}
III	1.62	7.6×10^{16}	10^{-8}	1×10^8	3.25×10^{11}	8.00×10^{-6}
IV	2.02	8.4×10^{19}	10^{-8}	8×10^8	2.00×10^9	5.00×10^{-8}
V	2.90	1.7×10^{27}	10^{-8}	1×10^8	3.25×10^{11}	6.00×10^{-6}
VI	1.38	5.3×10^{11}	10^{-8}	1×10^8	3.25×10^{11}	2.00×10^{-6}
NS1	4.20	1.0×10^{10}	10^{-8}	1×10^8	4.00×10^{11}	3.00×10^{-4}
NS2	3.20	1.0×10^{10}	10^{-8}	8×10^8	5.00×10^9	1.15×10^{-4}
NS3	2.20	5.3×10^{11}	10^{-8}	8×10^8	9.50×10^9	3.00×10^{-4}

structure of the TL material. With this purpose TXRD measurements of unirradiated samples and XRD measurements of irradiated samples using different values of absorbed dose have been made looking for differences between the diffractograms to determine the potential damage due to radiation exposure or thermal treatment i.e.: i) different peaks created during the irradiation or heating stages due to phase transitions; ii) changes in the intensity of the peaks due to possible amorphization process, as it may happened when the lattice is heating. Both i) and ii) could be the responsible of significant changes in the TL glow curves.

As it can be seen in Fig. 4, The TXRD patterns do show neither new peaks nor strong variations in crystallinity, (but minor changes due to heating process). In addition, XRD patterns (Fig. 3) do not show evidences of new phase transitions that can be observed in the irradiated samples.

Concerning the analysis of the TXRD patterns, the lithium fluoride crystalline structure can be described as two interpenetrated face-centred cubic lattice (fcc), where each cation is surrounded by 6 anions and vice versa, so the observable XRD peaks are due to those planes with Miller index are all odd or all even, so the crystallinity index can be written as follow:

$$\mathrm{CrI} = \left[1 - \frac{I_i}{I_{max}}\right] \times 100 \tag{3}$$

TL emission is produced by the radiative recombination of free electrons in the conduction band and trapped holes in the recombination centres. Thus, the TL intensity, in case of linear heating with heating rate β, the TL intensity is:

$$I_{TL}(T) = \frac{1}{\beta} A_{nm} \; m \; n_c \tag{4}$$

During the heating processes, the increase of free electrons density in de conduction band, n_c, is due to the thermal release of electrons previously trapped during the irradiation of the material. According to equation (1), the release rate from every trap, $\dot{n}_i$, depends on the products $p_i n_i$ and $A_i(N_i\text{-}n_i)n_c$, thus it could be strongly affected by variations in the total density of electron trapping centres, Ni, either produced during irradiation or heating processes.

The differential equation system (1) has been numerically solved, using equation (2) to describe the increase of the number of trapping and recombination centres during irradiation. In order to determine the most adequate parameters values for the model, an exhaustive set of simulations have been performed, increasing the number of trapping centres and varying the kinetic parameters looking to reproduce the LiF:Mg,Cu, P behaviour in the high temperature range (as it is displayed in Fig. 2). Thus, a system consisting of 9 electron trapping centres, a radiative recombination centre and a non-radiative centre has been considered in detail. The kinetic parameters for the trapping centres (E, s, A) and those that describe its growth during irradiation (N_0, N_{Sat}, C) are listed in Table 1. For the radiative recombination centre, the kinetic parameters are $E_h = 3.20$ eV, $s_h = 1.0 \times 10^{10}$ s^{-1}, $A_h = 1.0 \times 10^{-7}$ $cm^{-3}s^{-1}$, $A_{mn} = 1.0 \times 10^{-8}$ $cm^{-3}s^{-1}$ and the parameters for equation (2) are $M_0 = 2.0 \times 10^{+8}$ cm^{-3}, $M_{Sat} = 6.0 \times 10^{+8}$ cm^{-3}, $C_M = 2.45 \times 10^{-4}$. For the non-radiative recombination centre, the kinetic parameters are $E_h' = 3.20$ eV, $s_h' = 1.0 \times 10^{10}$ s^{-1}, $A_h' = 1.0 \times 10^{-11}$ $cm^{-3}s^{-1}$, $A_{mn}' = 1.0 \times 10^{-8}$ $cm^{-3}s^{-1}$and the parameters for equation (2) are $M_0' = 1.0 \times 10^{8}$ cm^{-3}, $M_{Sat}' = 1.0 \times 10^{9}$ cm^{-3}, $C_M = 3.0 \times 10^{-5}$.

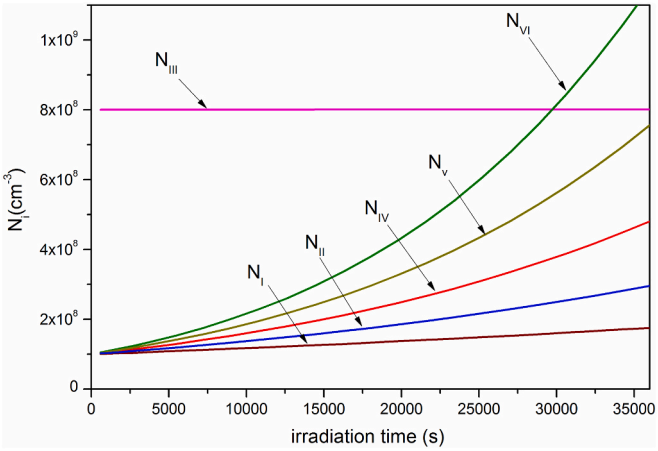

Fig. 5. Growth of the density of trapping centres, N_i, with the irradiation time.

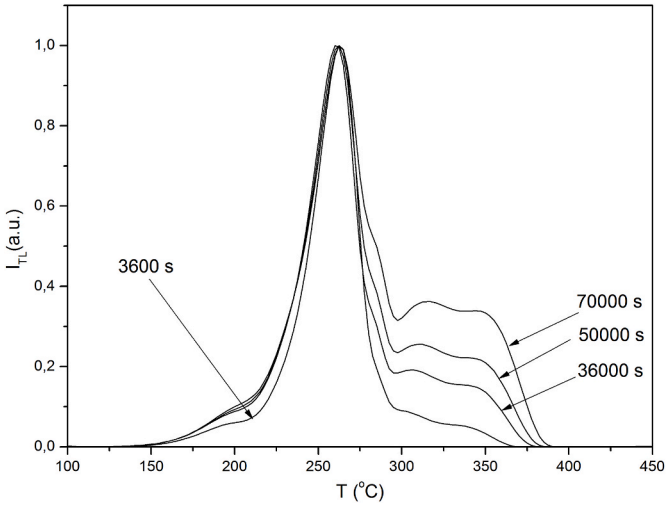

Fig. 6. Simulated TL glow curves, according to the model described in section 2.

The trapping centres identified with roman numbers I to VI permit to reproduce qualitatively the behaviour of the LiF:Cu,Mg,P glow curve response. The trapping centres labelled N_{S1}, N_{S2} and N_{S3} act as electron sinks during the heating process (Benavente et al., 2020).

Fig. 5 shows the variation of the total density of electron trapping centres N_I - N_{VI}, during irradiation, according to the model described by equation (2) and the parameters listed in Table 1. As is observed, all $N_i(t)$ values grow as the irradiation time increases; however in order to qualitatively reproduce the experimental results shown in Fig. 2, the growth parameters were defined to emphasize this phenomenon over the high temperature traps, keeping the Absorbed Dose Response (linear followed by sub-linear area) previously described; This introduces modifications over the electrons trapping capabilities, used in equation (1) through the term $A_i(N_i\text{-}n_i)$ that now depends on the irradiation time (i.e. the absorbed dose). As a consequence, the glow curve shape for rising irradiation time change significantly, producing a gradual increase in the high temperature peaks without affecting the most intense peak and the low temperature region, as it is illustrated in Fig. 6.

The situation can be better understood in Fig. 7, where time variation

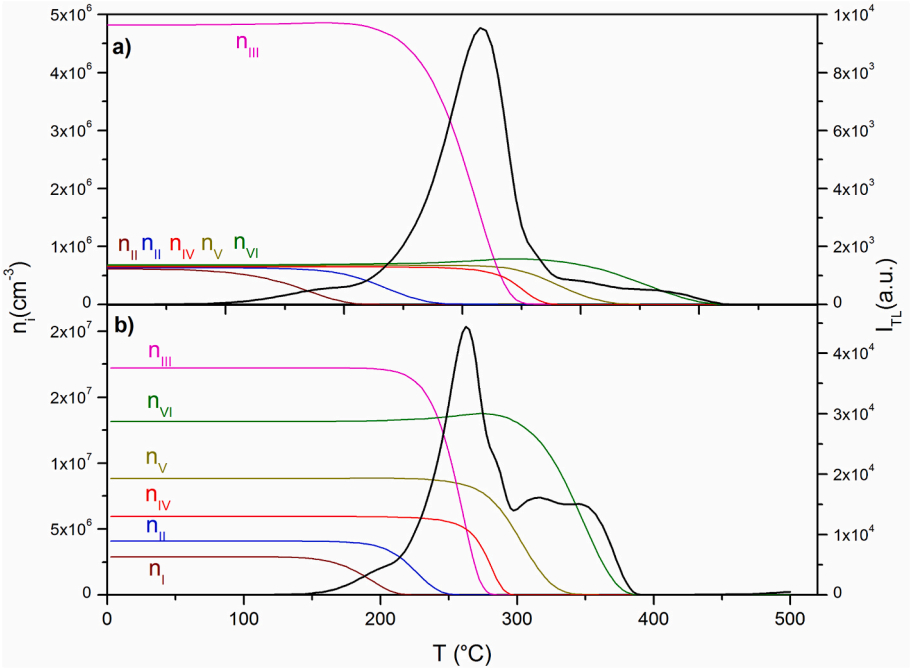

Fig. 7. Simulated TL glow curves (right axis) and temperature variation of the density of trapped electrons (left axis) for (a) the shorter and (b) the largest irradiation times considered.

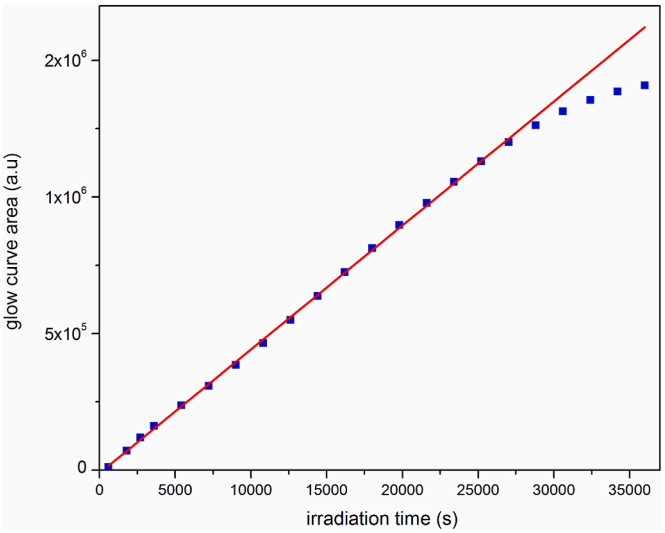

Fig. 8. Simulated TL response function: glow curve area versus irradiation time.

of the electron concentrations in the trapping centres I - IV during readout, $n_i(t)$, are shown together with the resulting glow curve, for the shorter (a) and larger (b) irradiation times considered in Fig. 6 (1.6×10^3 and 10^5 s, respectively). The differences in the $n_i(t)$ variations arising from different values of N_i, corresponding to different irradiation times, cause strong different in the TL glow curve shapes.

The simulation of the glow curves carried out with the appropriate set of parameters also reproduces the experimentally observed absorbed dose response (linear followed by sub-linear), as it is shown in Fig. 8 displaying the glow curve area as a function of the irradiation time. Assuming that absorbed dose is proportional to the irradiation time, this dependence agrees with the experimentally measured response (Moscovitch and Horowitz, 2007; Ginjaume et al., 1999).

During both irradiation and readout (heating) steps, the density of free electrons in the conduction band is the result of competition between trapping rate, governed by $\Sigma A_i(N_i\text{-}n_i)$, and recombination rate, expressed as $A_{mn}m$. For the shorter irradiation times, recombination compensates retrapping in sink traps (linearity area) until the density of recombination centres, M, approaches the saturation value (sub-linearity area).

4. Conclusions

The XRD patterns do not show evidences about phase transitions that could have been induced in LiF:Mg,Cu,P during the heating or irradiation stages. Similarly, the TXRD patterns do not show evidences of amorphization in the crystalline lattice that could have been produced during the heating process. So that, kinetic model combining the TL differential equation system and sigmoid-type dependence for the creation of trapping/recombination centres during irradiation has been introduced. This model qualitatively reproduces the observed behaviour and dose response of LiF:Mg,Cu,P when it is irradiated to absorbed dose values in the order of kGy.

CRediT authorship contribution statement

J.F. Benavente: Conceptualization, Methodology, Formal analysis, Software, Data curation, Writing - original draft. **J.M. Gómez-Ros:** Validation, Writing - review & editing, Supervision, Project administration, Funding acquisition. **V. Correcher:** Visualization, Investigation, Writing - review & editing.

Declaration of competing interest

The authors declare that they have no known competing financial interests or personal relationships that could have appeared to influence the work reported in this paper.

References

Benavente, J.F., Gómez-Ros, J.M., Romero, A.M., 2020. Numerical analysis of the irradiation and heating processes of thermoluminescent materials. Radiat. Phys. Chem. 170, 108671.

Bilski, P., Obryk, B., Olko, P., Mandowska, E., Mandowski, A., Kim, J.L., 2008. Characteristics of LiF:Mg,Cu,P thermoluminescence at ultra-high dose range. Radiat. Meas. 43, 315–318.

Carella, E., Hernández, T., 2015. The effect of -radiation in Li4SiO4ceramic breeder blankets. Fusion Eng. Des. 90, 73–78.

Cheney, W., Kincaid, D., 2002. Numerical Analysis: Mathematics of Scientific Computing. Texas University.

Dauletbekova, A., Schwart, K., Dorokin, M.V., Russakova, A., Baizhumanov, M., Akilbekov, A., Zdorovets, M., Koloberdin, M., 2014. F center creation and aggregation in LiF crystals irradiated with ^{14}N, ^{40}Ar and ^{84}Kr ions. Nucl. Instrum. Methods B. 326, 311–313.

Epie, E.N., Wijesundera, D.N., Tilakarante, B.P., Chen, Q.Y., Chu, W.K., 2016. Rate of F center formation in sapphire under low-energy low-fluence Ar^{+} irradiation. Nucl. Instrum. Methods Phys. Res. B 371, 303–306.

García-Cortés, I., Malo, M., Moroño, A., Muñoz, P., Valdivieso, P., Hodgson, E., 2018. In-situ evaluation of radiation induced optical degradation of candidate scintillator materials for ITER's gamma and neutron detectors. Fusion Eng. Des. 136, 493–497.

Ginjaume, M., Ortega, X., Duch, M.A., Jornet, N., Sanchez Reyes, A., 1999. Characteristics of LiF:Mg,Cu,P for clinical application". Radiat. Protect. Dosim. 85 (1–4), 389–391.

McKeever, S.W.S., 1985. Thermoluminescence of Solids. Cambridge University Press, London.

Moscovitch, M., Horowitz, Y.S., 2007. Thermoluminescent materials for medical applications: LiF:Mg,Ti and LiF:Mg,Cu,P. Radiat. Meas. 41, S71–S77.

Schuldman, J.H., Compton, W.D., 1963. Color Centers in Solids, ume 2. Pergamon Press, London.